ATGP copy

AFRRI SR75-8
APRIL 1975

AFRRI
SCIENTIFIC
REPORT

A QUALITATIVE AND QUANTITATIVE COMPARATIVE ANALYSIS OF SCINTILLATION CAMERA TOMOGRAPHY WITH THE LATEST CONVENTIONAL IMAGING TECHNIQUES

V. L. McManaman
M. D. Sinclair

ARMED FORCES RADIOBIOLOGY RESEARCH INSTITUTE
Defense Nuclear Agency
Bethesda, Maryland

AFRRI SR75-8

AFRRI SR75-8
April 1975

A QUALITATIVE AND QUANTITATIVE COMPARATIVE ANALYSIS OF SCINTILLATION CAMERA TOMOGRAPHY WITH THE LATEST CONVENTIONAL IMAGING TECHNIQUES

V. L. McMANAMAN
M. D. SINCLAIR

ANDREW P. BLASCO
Lieutenant Colonel, USA
Acting Chairman
Radiation Biology Department

MYRON I. VARON
Captain MC USN
Director

ARMED FORCES RADIOBIOLOGY RESEARCH INSTITUTE
Defense Nuclear Agency
Bethesda, Maryland

ACKNOWLEDGMENT

The authors express their appreciation to N. L. Fleming, J. K. Warrenfeltz, E. L. Barron and M. E. Flynn for their outstanding support and enthusiasm in acquiring the experimental data; to E. E. Sereno and W. E. Jackson for their extensive contributions in the development of the computer programs; to Dr. A. Strash and the computer staff at the Medical College of Virginia for developing the PL/I job control language; and to J. S. Stevenson who provided considerable advice, support, and encouragement throughout this undertaking.

TABLE OF CONTENTS

LIST OF FIGURES

TABLE

FOREWORD
(Nontechnical summary)

The rapid growth of the field of nuclear medicine over the past several years can be attributed primarily to the development by Dr. H. O. Anger of the scintillation camera for generating images of radionuclides distributed throughout the organs of the body. The scintillation camera is much faster and more versatile than the older rectilinear scanner. The development of the scintillation camera has resulted in many modifications and adaptions to meet a variety of clinical requirements. Two such new devices, a tomographic unit and a DIVCON collimator, recently acquired by the AFRRI were comparatively evaluated with respect to well-established imaging instruments including the pinhole collimator, the high resolution collimator, the high sensitivity collimator, the rectilinear scanner and computer processed images.

The tomography attachment (Tomocamera) to the scintillation camera allows the generation of five images simultaneously where each image is effectively focused at a different depth within the organ under consideration. According to the degree of focus, the depths of tumors or other defects may then be determined without the need for acquiring additional views (i.e., lateral, posterior-anterior, etc.). The major advantages of the tomographic unit are speed and possibly increased resolving power.

The DIVCON collimator is essentially a combination high resolution-high sensitivity magnifying collimator designed to combine the advantages of the high resolution and high sensitivity collimators.

Through the use of special head and tumor phantoms designed to challenge the detection limits of all the systems mentioned, qualitative comparisons were performed

using the film images. They reveal the following order of performance in decreasing sequence: rectilinear scanner, pinhole collimator, DIVCON collimator, high resolution collimator and Tomocamera. Computer images for all the camera systems are comparable in quality to that of the rectilinear scanner. Quantitative data (viz., resolution indices and modulation transfer functions) for the scintillation camera systems were obtained from computer images of a uniform line source of activity. These demonstrate the following responses in decreasing order: DIVCON collimator, high resolution collimator, Tomocamera and high sensitivity collimator. These quantitative data show a wider margin of difference in response of the systems, thereby supporting the need for their use as a more sensitive criterion for evaluating imaging systems.

Although the quantitative data are complete and rigorous, considerable phantom and patient data are still required for a more thorough applied or clinical evaluation of these systems. Particular emphasis should be given to cases where the tissue surrounding the tumor or defect has a higher specific activity than the tumor itself.

ABSTRACT

Since very little objective information is available on the image quality and operating performance of a commercially available scintillation camera tomography attachment (Tomocamera) and a new combination high resolution-high sensitivity magnifying scintillation camera collimator (DIVCON), a study was undertaken to perform a comparative analysis on the response of these two systems with the well-known high resolution and high sensitivity collimators as well as with the pinhole collimator, rectilinear scanner and computer processed images recorded from the camera. Qualitatively the image data of the Alderson head phantom containing a barely detectable tumor phantom indicate that the order of quality decreases in the following sequence: rectilinear scanner, pinhole collimator, DIVCON collimator, high resolution collimator and Tomocamera. Computer processed images using the latter three collimators render quality as good as that of the rectilinear scanner. A quantitative evaluation using resolution indices and modulation transfer functions shows that the response quality decreases in the following sequence: DIVCON collimator, high resolution collimator, Tomocamera and high sensitivity collimator. Although the quantitative data support the qualitative data, it is shown that the quantitative method reveals greater margins of difference and thus is a much more sensitive indicator of the response of these systems.

I. INTRODUCTION

The rapid growth of clinical nuclear medicine includes the development of new and quite sophisticated instrumentation for imaging. The scintillation camera which has been widely used for the past decade provides the most powerful means of generating images of radionuclide distributions and accounts almost exclusively for the rapid development of clinical nuclear medicine. Continuing improvements and adaptations to the basic scintillation camera are being made by commercial manufacturers and private research groups. Both are expending considerable effort on the development of new collimators for a variety of specific applications. However, thorough clinical evaluations of these collimators are usually delayed and often inadequate due to rather inflexible patient schedules of busy nuclear medicine clinics. As a result, an evaluation of several of the latest collimator systems was undertaken at the AFRRI where experimental control and rigor could be exercised unimpeded by the numerous constraints experienced in the hospital clinics.

A tomographic imaging device[4,5] and a new combination high resolution-high sensitivity magnifying collimator[6] were evaluated and compared quantitatively with the standard high resolution and high sensitivity collimators and qualitatively with the pinhole collimator and rectilinear scanner. Although some information is available in the literature,[2,3] there has been no comprehensive evaluation of these devices with respect to well-established techniques.

II. MATERIALS AND METHODS

The instrumentation associated with the tomography system (Tomocamera) includes a collimator with slanted parallel holes which is attached to the standard

Nuclear-Chicago Pho/Gamma HP scintillation camera and which rotates synchronously with a table positioned beneath the camera detector. Through this synchronous rotation and considerable electronic circuitry, five diffcrent images of a given organ are generated simultaneously with each image focused at a different depth within the organ. The purpose of such a system is to simultaneously provide visualization and depth approximation of defects by recording a single view in contrast to the time-consuming multiple views normally recorded with stationary camera systems. One of the five images corresponds to a predetermined depth called the geometric focal plane (GFP), while the remaining four images correspond to depths called tomoplanes and are determined by the GFP setting and a control to vary the distance between tomoplanes. The depth of the GFP which is set by an armature beneath the rotating table is directly proportional to the diameter of rotation of the table. A variety of settings for revolution rate and total number of revolutions of the collimator and table are available for terminating studies. The four tomoplane images are simultaneously displayed on a single cathode-ray tube (CRT) while the GFP image is displayed singly on a second CRT. Tomographic data which are recorded on videotape may be replayed with completely different tomoplane settings in order to generate additional images corresponding to other organ depths.

The new combination high resolution-high sensitivity magnifying collimator (DIVCON) was developed by Nuclear-Chicago to provide a spatial resolution similar to that of the high resolution collimator and a sensitivity similar to that of the high sensitivity collimator to produce well resolved images in a relatively short imaging time. The collimation holes of the DIVCON are in a focusing configuration as opposed to the

straight parallel configuration of the other two collimators. The focused holes serve to increase sensitivity as well as to provide a magnified image.

The qualitative evaluation of these devices was accomplished by imaging an Alderson head phantom with a volume of 3500 cm^3 and containing a pseudotumor with a volume of 6 cm^3. Both phantoms were filled with water and technetium-99m in saline solution at such a volume normalized tumor to tissue activity ratio to produce a barely discernible image of the tumor on Polaroid film taken from the scintillation camera console CRT. Once the proper activity ratio was obtained the phantoms were immediately imaged using all of the collimators and the rectilinear scanner (Picker Magnascanner). Except for the rectilinear scanner all images were recorded simultaneously by the Nuclear Data MED-II computer in a 64 x 64 matrix. The computer images received some processing and were compared qualitatively with the CRT images from the scintillation camera console.

The quantitative evaluation which includes the Tomocamera, the DIVCON, the high resolution and high sensitivity collimators was performed by recording, with the computer, the camera images of a thin line source of activity (Figure 1A) placed at various positions across the surface of the scintillation camera detector as well as at various depths of water. Profile slices (Figure 1B and C) across the resulting digital images were fitted with mathematical functions which included a central Gaussian distribution and two exponential distributions for the outer tails. That is, raw data profile slices which were computer corrected for nonuniformities in sensitivity response across the surface of the detector (flood field correction) were fitted to the general mathematical function

$$y(x) = A_1 \ell^{-B_1 x} + A_2 \ell^{-(x-\bar{x})^2/2\sigma^2} + A_3 \ell^{-B_2 x} \quad (1)$$

where $\bar{x}$ = peak centroid and σ = peak standard deviation. A computer program provided fitted values for A_1, A_2, A_3, $\bar{x}$, σ, B_1 and B_2 and selected the optimum change-over points between the different functions. From these parameters two evaluations, resolution index and modulation transfer function,[1] were made which demonstrate the

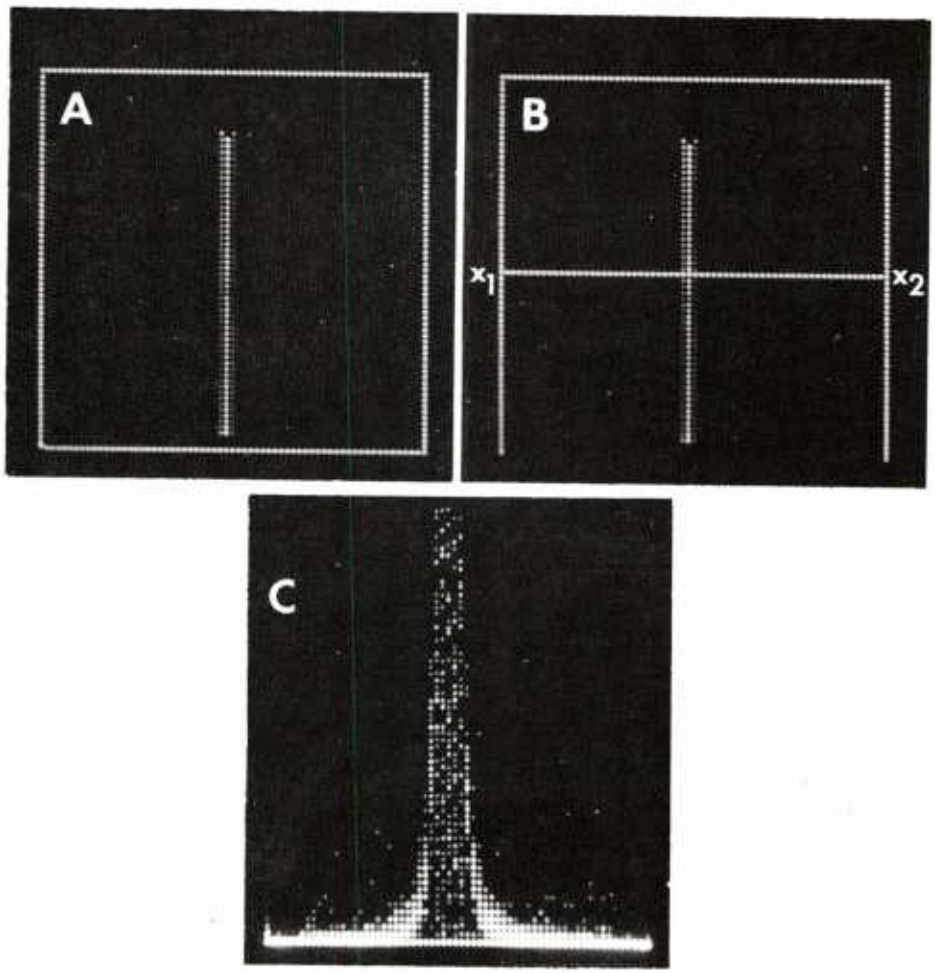

Figure 1. Computer planar image of line source of activity (A). Profile slice x_1, x_2 across image (B) provides raw data for generating line spread function L (χ) (C).

integral response quality of the particular collimator and scintillation camera systems. The resolution index is the value of the full width at half the peak (FWHM) value of the central Gaussian distribution and is related to the standard deviation (σ) by a constant. If the response of a system is truly represented by a Gaussian distribution, then the FWHM value adequately suffices as an indicator of the system quality. However, this is frequently not the case particularly when a scattering medium is present. Two distributions (Figure 2) may have identical FWHM values and radically different tail distributions. Such occurrences are taken into account by an evaluation of the MTF for the entire distribution including the tails. Basically the MTF is a measure of the reproduction fidelity of a detector system to a well-defined object to be imaged. For example, the object modulation (m_o) (Figure 3, object) is defined mathematically as $m_o = \frac{\hat{y}}{\bar{y}}$ where $\hat{y}$ is a measure of the variation of a function $y(x)$ from a biased level $\bar{y}$. The image pattern may be similarly represented by the image modulation $m_i = \frac{\hat{z}}{\bar{z}}$ (Figure 3, image). The ratio of the image modulation to the object modulation is the MTF, that is $\text{MTF} = \frac{m_i}{m_o}$ so that for an image which is a perfect reproduction of an object the MTF value is one.

It has been shown that the mathematical function $L(\chi)$ (line spread function) describing the profile slice of a line source of activity (Figure 1C) can be used to evaluate the MTF of a system through the equation

$$\text{MTF}(u) = \frac{\int_{-\infty}^{\infty} L(\chi)\, e^{-2\pi i u \chi} d\chi}{\int_{-\infty}^{\infty} L(\chi)\, d\chi} \qquad (2)$$

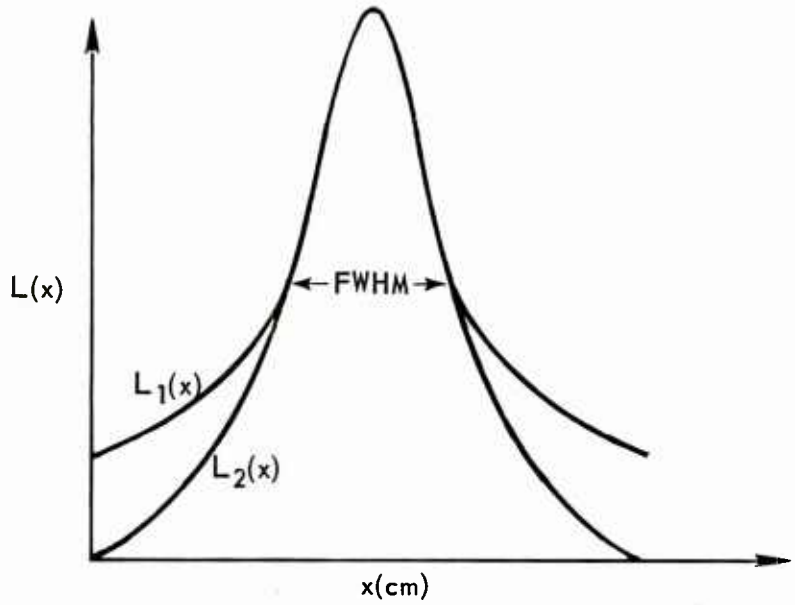

Figure 2. Two line spread distributions with same resolution index provide different MTF distributions

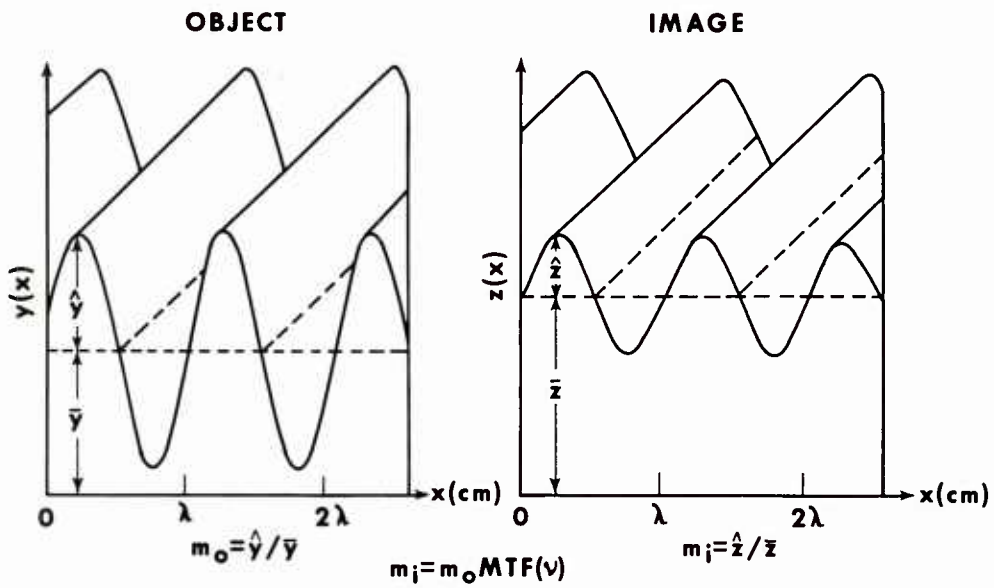

Figure 3. Transfer of modulation of an object m_o to modulation of its image m_i defines MTF for a given spatial frequency

which is simply the inverse Fourier transform of the function L (χ) normalized so that at $\mu = 0$, MTF = 1. If L (χ) is an even function as is usually the case, equation (2) reduces to

$$\text{MTF}\ (\mu) = \frac{\int_{-\infty}^{\infty} L\ (\chi)\ \cos\ 2\Pi\mu\chi\ d\chi}{\int_{-\infty}^{\infty} L\ (\chi)\ d\chi} \tag{3}$$

and is written numerically as,

$$\text{MTF}\ (\mu) = \frac{\Sigma_i\ L\ (\chi i)\ \cos\ 2\Pi\mu\chi i}{\Sigma_i\ L\ (\chi i)} \quad . \tag{4}$$

The experimental configuration to obtain both the resolution index and the MTF included a thin polyethylene tubing (inside diameter of 1.1 mm) filled with technetium-99m and fitted for support into a slot along a thin strip of Lucite. The line source was placed at various depths and lateral positions in air and in water beneath the detector. Multiple images at each location were acquired by the MED-II computer for good counting statistics since the maximum value of any element of the 64 x 64 matrix was 4096. Due to the large volume of such data a special computer program was developed to transfer the data via magnetic tape to the National Institutes of Health IBM-360 computer system which rapidly summed the matrices and provided a printed copy of the resultant matrix. Although the magnetic tape was mechanically compatible between the MED-II and the IBM-360 computers, a programming difficulty was encountered as the result of the data packing format of the 12-bit words by the MED-II magnetic tape system. Each 12-bit word occupies eight tracks of one

magnetic tape channel plus four tracks of the next channel. However, instead of starting the next sequential word in the next empty channel, the first four bits are stored in the remaining four empty tracks of the previous channel while the last eight bits fill the channel after that. Since the Fortran languages are not capable of separating this type of packed information, a high level language (PL/I) was found that could be used to read data from magnetic tape bit by bit rather than channel by channel. The PL/I language which is far more powerful than Fortran is basically a combination of the Fortran, Cobal and Algol languages. As a result all data processing associated with magnetic tape input data on the IBM-360 is carried out in PL/I. Profile slices of the resultant summed data are then used in another Fortran program executed on the AFRRI SDS-920 computer system to obtain the parameters of the mathematical function, equation (1), to which the data are fitted. A final computer program was then developed which used these parameters to evaluate all MTF's.

III. RESULTS

Before considering the comparative data for the head and tumor phantoms, two examples are given which demonstrate the need for extreme caution in the interpretation of tomographic images. Transmission images of a bar phantom using the Tomocamera were recorded (Figure 4A and B) and in both cases the distance between the detector and bar phantom is the same and only the GFP setting has been changed. In one case (Figure 4A) the image in best focus is tomoplane 1 while tomoplanes 2, 3 and 4 represent distances increasingly farther away from the plane where the actual phantom is located and yield defocused images. With a different GFP setting (Figure 4B) the image in best focus is now tomoplane 4 with tomoplanes 3, 2 and 1 representing

Figure 4. Planes of focus 1 (A) and 4 (B) for same collimator to source distance and different GFP control settings for Tomocamera

increasingly greater distances from the plane where the actual phantom is located and again yield defocused images. These two examples demonstrate that focused data in any of the tomoplanes are direct functions of the GFP settings, so that only if the system is carefully operated and calibrated can the depth of a defect be determined. Further, by observing the change in focus of the lower right quadrant of the bar phantom in Figure 4A and the upper right in Figure 4B for sequentially greater distances away from the tomoplane of best focus, it is apparent that these quadrants come back into focus at the most distant tomoplane rather than continuing to greater defocusing as would be expected. The explanation for this refocusing is that the width of the lead bars in the applicable quadrants is equivalent to approximately half the distance which the data are shifted when they are processed by the Tomocamera electronics. For practical clinical situations particularly where the radionuclide distribution is unknown, data shifting can lead to erroneous estimates of defect depths as well as to the generation of artifacts. A striking demonstration of artifact generation is exhibited by imaging a point source using the same experimental parameters as for the bar phantom (Figure 5A). A well focused point source in tomoplane 1 (Figure 5A) also reveals an

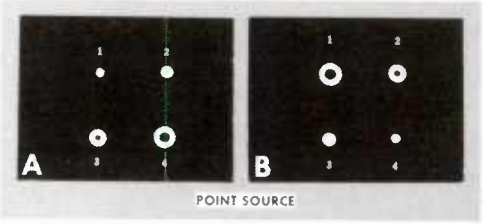

Figure 5. Artifacts 2, 3 and 4 (A) and 1, 2 and 3 (B) generated by Tomocamera imaging point source 1 (A) and 4 (B) for same collimator to source distance and different GFP control settings

artifactual annular image in tomoplane 4. The same artifact occurs in tomoplane 1 when the GFP is reset to place the image of best focus in tomoplane 4 (Figure 5B). Again when the radionuclide distribution within an organ is not known as is nearly always the clinical situation, grave errors can occur from deceptive artifacts which appear within the image.

Images of the head (with skull) and tumor phantoms were recorded where the tumor was located 2 in. beneath the surface of the head at a tumor to tissue volume normalized activity ratio of 3.3 (Figure 6). Qualitatively the rectilinear scanner image (Figure 6D) in this case provides the best view of the tumor while the pinhole collimator yields the next best view (Figure 6C). Tumor definition provided by the high resolution collimator (Figure 6B) and Tomocamera (Figure 6A) appears to be approximately equivalent but somewhat worse than that provided by the rectilinear scanner and the pinhole collimator. Interestingly, the computer displays of the Tomocamera (Figure 6E), the high resolution collimator (Figure 6F) and pinhole collimator (Figure 6G) all provide images of the tumor which are superior to the scintillation camera console CRT images and which are also approximately equivalent to the quality of the rectilinear scanner image.

The same procedure was repeated after lowering the tumor phantom to 3 in. beneath the surface of the head phantom and increasing the activity ratio to 3.5. Again the rectilinear scanner provided the best tumor image (Figure 7D) while the image

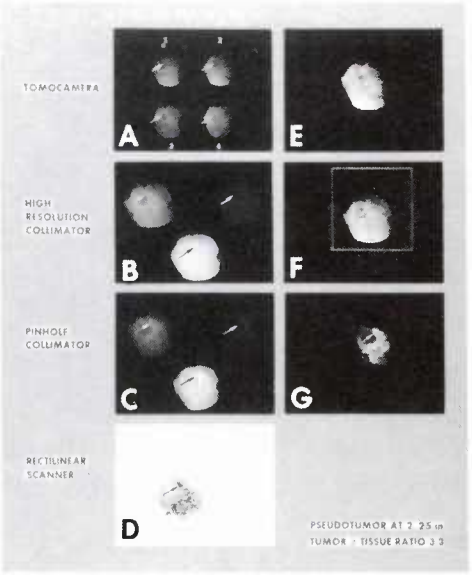

Figure 6. Head and tumor (†) phantom images recorded with Tomocamera (A), high resolution collimator (B), pinhole collimator (C) and rectilinear scanner (D) with corresponding computer displays (E, F and G) for tumor at 2.25 in. from collimator and activity ratio of 3.3

qualities of the pinhole collimator (Figure 7C) and the high resolution collimator (Figure 7B) sequentially decreased. The tumor was barely discernible with the Tomocamera (Figure 7A). Once again the computer displays for the pinhole (Figure 7F) and high resolution (Figure 7E) collimators yield a tumor image quality superior to that

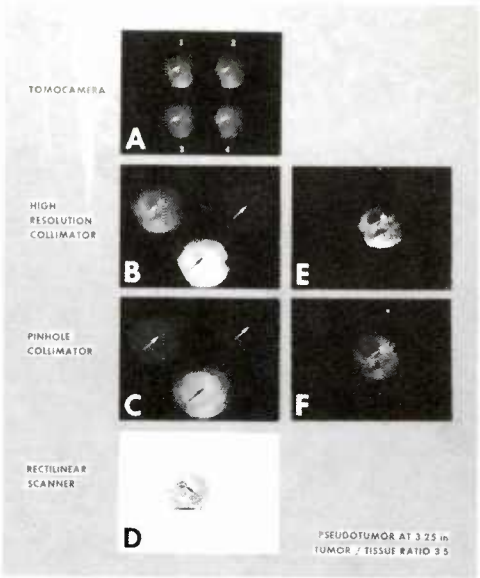

Figure 7. Head and tumor (r) phantom images recorded with Tomocamera (A), high resolution collimator (B), pinhole collimator (C) and rectilinear scanner (D) for tumor at 3.25 in. from collimator and activity ratio of 3.5

obtained from the standard scintillation camera console CRT images and approximately equivalent to that of the rectilinear scanner image.

The DIVCON collimator, which was acquired after the completion of the previous qualitative evaluation, was compared with the high resolution collimator by imaging the Alderson head (without skull) and tumor (volume of 6 cm^3) phantoms. With the tumor at 3 in. beneath the surface of the head and using a volume normalized tumor to tissue activity ratio of 2.5 the tumor could not be visualized with the high resolution collimator (Figure 8A). However, with some uncertainty the tumor may be visualized

with the DIVCON collimator (Figure 9A). The computer displays after some data processing including a flood field correction yielded an easily discernible tumor for both collimators (Figures 8C and 9C).

The quantitative evaluation resulted in the resolution indices with standard deviations shown in Table I for various depths of air and water. Each value represents the average of approximately nine points over the detector. Although the values for the DIVCON collimator are only slightly lower than those for the high resolution

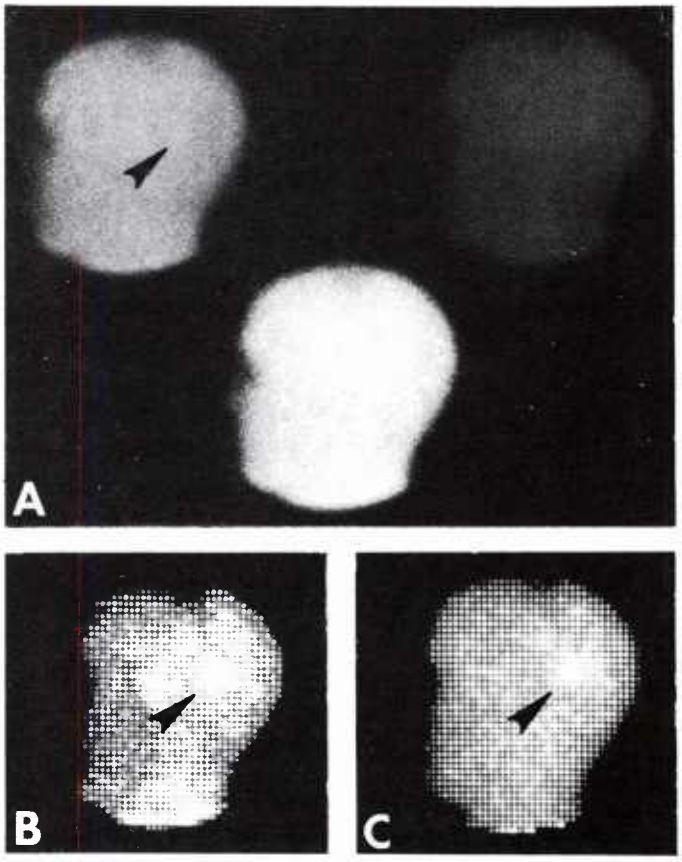

Figure 8. Normal scintillation camera console CRT image (A) using high resolution collimator reveals no discernible tumor while computer image (B) after simple processing reveals clearly discernible tumor image (C) (7)

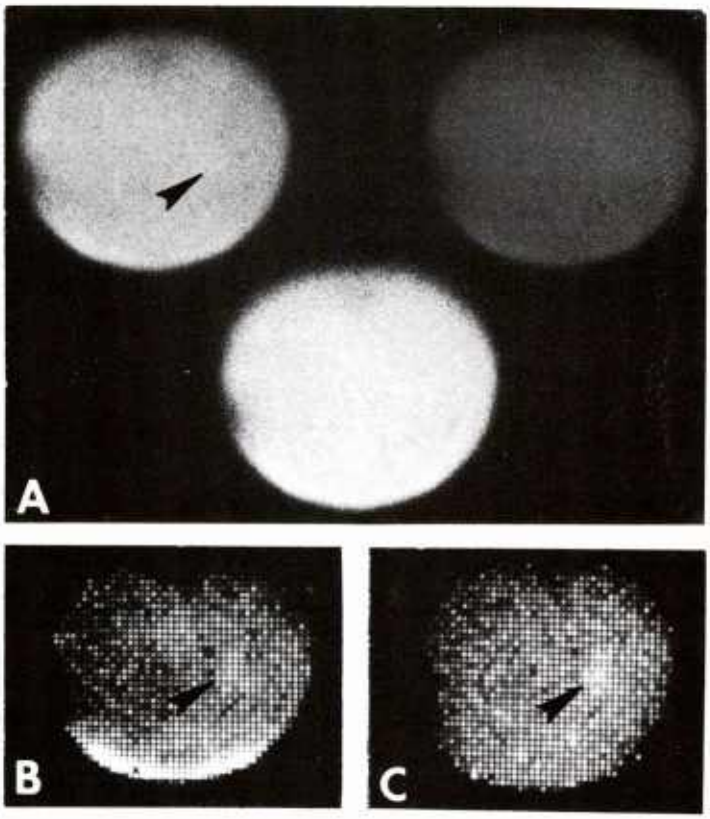

Figure 9. Normal scintillation camera console CRT image (A) using DIVCON collimator reveals barely discernible tumor (↗) while computer image (B) after simple processing reveals clearly discernible tumor (C) (↗)

Table I. Resolution Indices and Standard Deviations for Four Collimator Systems for Air and Water Scattering Media

	High resolution	DIVCON	Tomocamera	High sensitivity
2 cm Air	9.31 ± .17	8.73 ± .30	10.34 ± .59	10.29 ± .28
2 cm Air + 2 cm H_2O	9.92 ± .20	9.59 ± .22	11.15 ± .26	11.49 ± .31
2 cm Air + 4 cm H_2O	10.72 ± .46	10.21 ± .17	12.57 ± .28	12.63 ± .43
2 cm Air + 6 cm H_2O	11.33 ± .45	11.11 ± .40	13.32 ± .46	14.31 ± .50
2 cm Air + 8 cm H_2O	12.18 ± .47	11.67 ± .55	14.58 ± .58	16.08 ± .89
2 cm Air + 10 cm H_2O	12.80 ± .50	13.07 ± .60	15.35 ± .82	17.76 ± 1.5

collimator the general response of the DIVCON can still be categorized as slightly better than that of the high resolution collimator since the former exhibits consistently lower resolution indices throughout the entire range of media thicknesses. A plot (Figure 10) of these resolution indices reveals practically parallel patterns for the DIVCON and high resolution collimators. The response of the Tomocamera is substantially inferior to these collimators and exhibits some divergence with increasing thickness of scattering media. Similarly the high sensitivity collimator response initially approximates that of the Tomocamera and strongly diverges with increasing thickness of scattering media. The MTF distributions for the four collimator systems

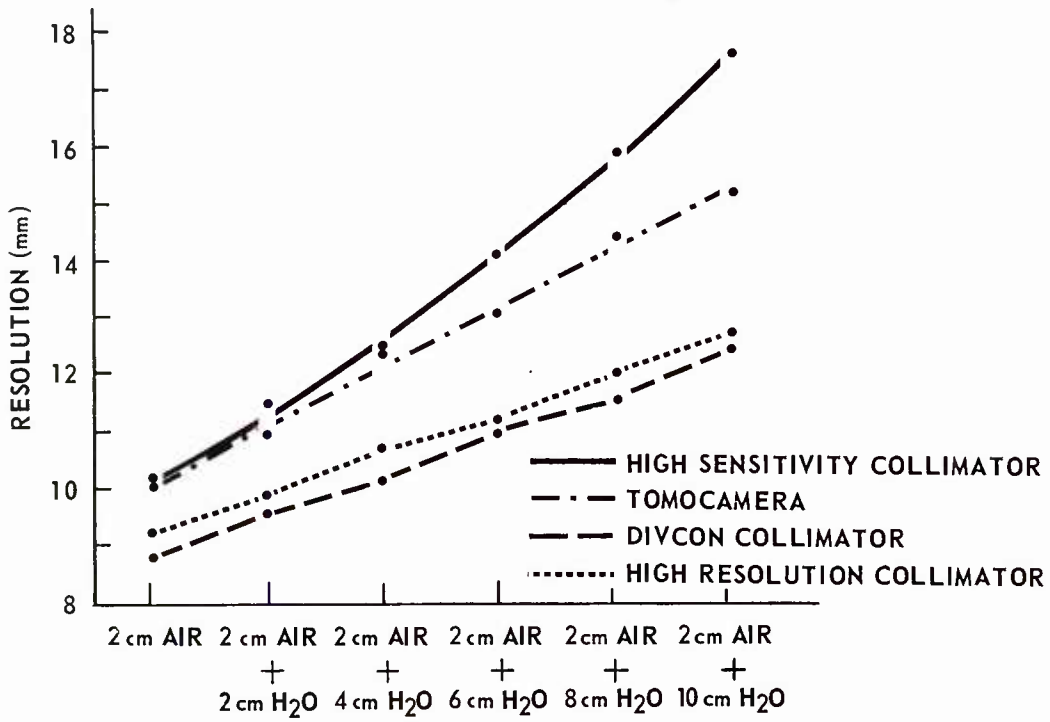

Figure 10. Graphic representation of data in Table I showing parallel response for high resolution and DIVCON collimators, some divergence for Tomocamera and considerable divergence for high sensitivity collimator at greater depths of media

are plotted for each depth of media in Figures 11 through 16. Like the resolution indices the MTF distributions indicate an approximately equivalent response for the DIVCON and high resolution collimators throughout the range of spatial frequencies and media thicknesses. The Tomocamera and high sensitivity collimator responses are approximately equivalent throughout the range of spatial frequencies for shallow depths of scattering media and diverge for increasing depths in agreement with the pattern followed by the resolution indices.

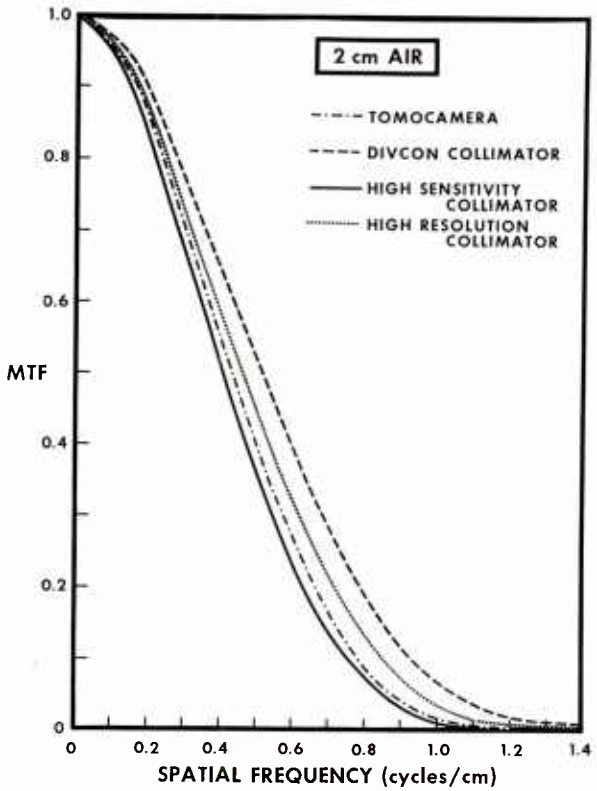

Figure 11. MTF distributions for four collimator systems for line source 2 cm of air beneath collimator

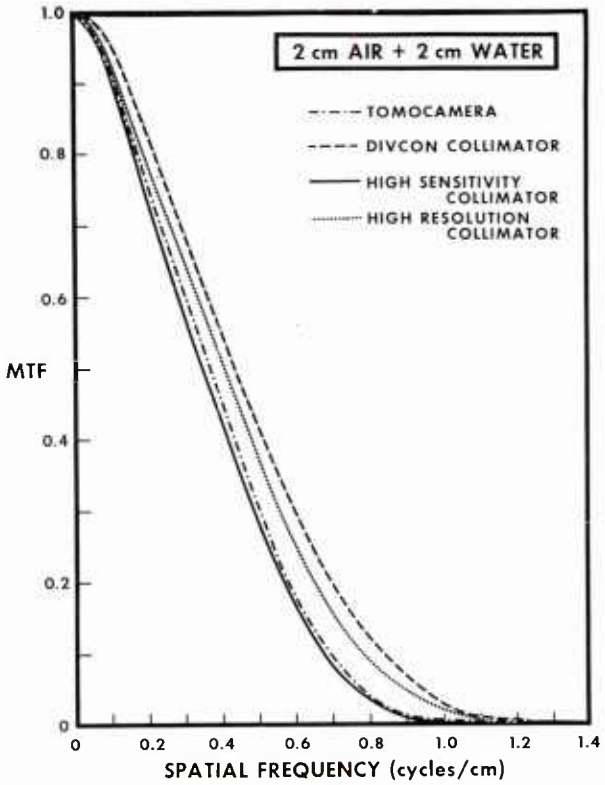

Figure 12.
MTF distributions for four collimator systems for line source 2 cm of air plus 2 cm of water beneath collimator

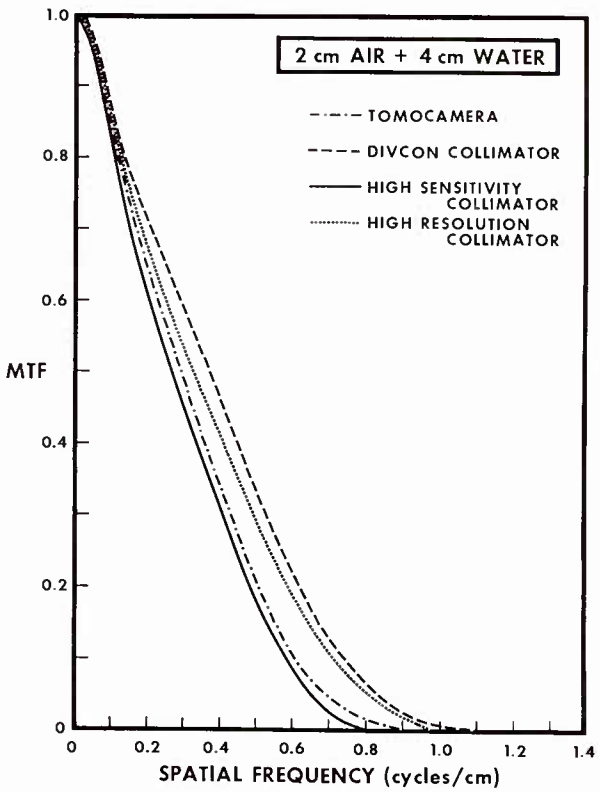

Figure 13.
MTF distributions for four collimator systems for line source 2 cm of air plus 4 cm of water beneath collimator

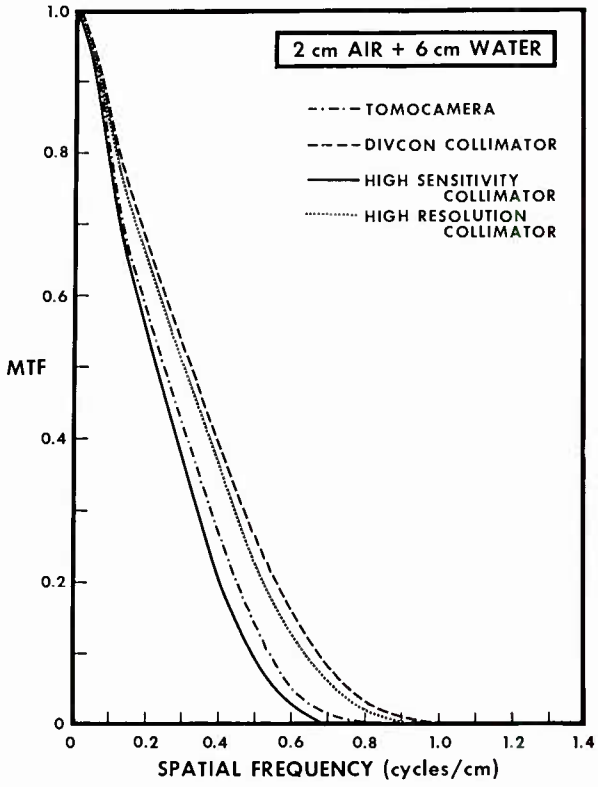

Figure 14.
MTF distributions for four collimator systems for line source 2 cm of air plus 6 cm of water beneath collimator

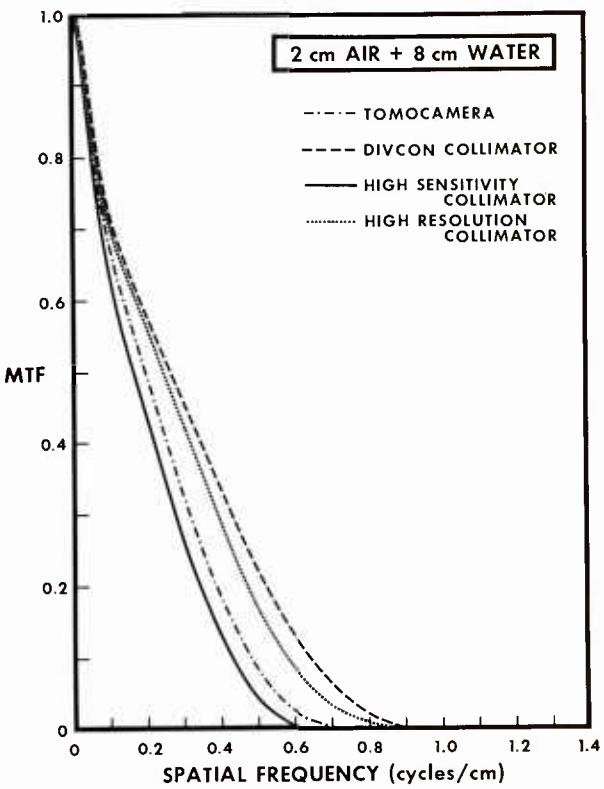

Figure 15.
MTF distributions for four collimator systems for line source 2 cm of air plus 8 cm of water beneath collimator

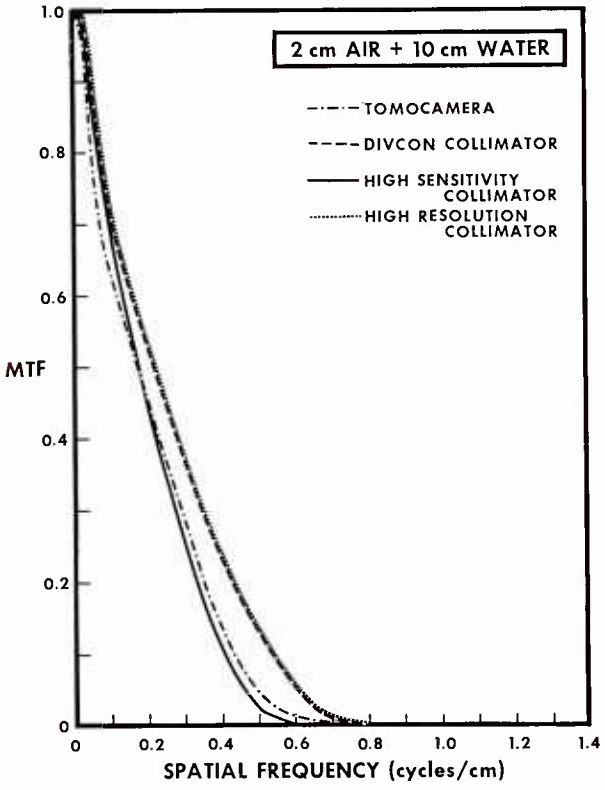

Figure 16. MTF distributions for four collimator systems for line source 2 cm of air plus 10 cm of water beneath collimator

IV. DISCUSSION

It has been shown that the qualitative phantom data and the quantitative mathematical data are in agreement for the Tomocamera, the high resolution collimator and the DIVCON collimator. The resolution indices for the DIVCON and high resolution collimators, although not substantially different, do demonstrate that the DIVCON collimator is slightly superior to the high resolution collimator (Figures 8 and 9). This difference is not as obvious in the phantom data where the DIVCON collimator had a barely perceptible advantage over the high resolution collimator. Based on the data from this particular phantom model and neglecting the rectilinear scanner,

the order of performance for the scintillation camera is: (1) pinhole collimator; (2) DIVCON collimator; (3) high resolution collimator; and (4) Tomocamera. On occasion the Tomocamera images equal but do not surpass the high resolution collimator data. The resolution indices and MTF values support this order of performance with a wider margin of difference thereby reinforcing the need for their use as a more sensitive criterion for evaluating system responses.

It should be noted that the phantom data presented here represent only one specific carefully controlled condition and should not be utilized as final criteria for categorizing a detector system. They should serve only as a first indicator of the quality of these particular detector systems. Although, the quantitative data are quite rigorous, a plethora of phantom configurations simulating many diverse organ systems needs to be investigated particularly for defects which have a tumor to tissue activity ratio of less than one.

REFERENCES

1. Beck, R. N. Modulation transfer function for radioisotope imaging systems. In: Handbook of Radioactive Nuclides, Wang, Y., editor, pp. 123-129. Cleveland, Ohio, The Chemical Rubber Company, 1969.

2. DeLand, F. H., James, A. E., Muehllehner, G. and Wagner, H. N., Jr. The value of tomography in liver scanning. Radiology 102:429-432, 1972.

3. Goldsmith, S. J. Image artifacts in tomographic gamma camera systems. J. Nucl. Med. 14:103-106, 1973.

4. Muehllehner, G. A tomographic scintillation camera. Phys. Med. Biol. 16:87-96, 1971.

5. Nuclear-Chicago Corporation. Publication Number 710-717050, Tomocamera. Des Plaines, Illinois, June 1971.

6. Nuclear-Chicago Corporation. Publication Number CM-299, DIVCON, Low Energy Collimator. Des Plaines, Illinois, July 1972.

UNCLASSIFIED
Security Classification

DOCUMENT CONTROL DATA - R & D

(Security classification of title, body of abstract and indexing annotation must be entered when the overall report is classified)

1. ORIGINATING ACTIVITY *(Corporate author)*
Armed Forces Radiobiology Research Institute
Defense Nuclear Agency
Bethesda, Maryland 20014

2a. REPORT SECURITY CLASSIFICATION
UNCLASSIFIED

2b. GROUP
N/A

3. REPORT TITLE
A QUALITATIVE AND QUANTITATIVE COMPARATIVE ANALYSIS OF SCINTILLATION CAMERA TOMOGRAPHY WITH THE LATEST CONVENTIONAL IMAGING TECHNIQUES

4. DESCRIPTIVE NOTES *(Type of report and inclusive dates)*

5. AUTHOR(S) *(First name, middle initial, last name)*
V. L. McManaman and M. D. Sinclair

6. REPORT DATE	7a. TOTAL NO. OF PAGES	7b. NO. OF REFS
April 1975	27	6

8a. CONTRACT OR GRANT NO.

b. PROJECT NO. NWED QAXM

c. Task and Subtask C 911

d. Work Units 08 and 09

9a. ORIGINATOR'S REPORT NUMBER(S)
AFRRI SR75-8

9b. OTHER REPORT NO(S) *(Any other numbers that may be assigned this report)*

10. DISTRIBUTION STATEMENT
Approved for public release; distribution unlimited

11. SUPPLEMENTARY NOTES

12. SPONSORING MILITARY ACTIVITY
Director
Defense Nuclear Agency
Washington, D. C. 20305

13. ABSTRACT

Since very little objective information is available on the image quality and operating performance of a commercially available scintillation camera tomography attachment (Tomocamera) and a new combination high resolution-high sensitivity magnifying scintillation camera collimator (DIVCON), a study was undertaken to perform a comparative analysis on the response of these two systems with the well-known high resolution and high sensitivity collimators as well as with the pinhole collimator, rectilinear scanner and computer processed images recorded from the camera. Qualitatively the image data of the Alderson head phantom containing a barely detectable tumor phantom indicate that the order of quality decreases in the following sequence: rectilinear scanner, pinhole collimator, DIVCON collimator, high resolution collimator and Tomocamera. Computer processed images using the latter three collimators render quality as good as that of the rectilinear scanner. A quantitative evaluation using resolution indices and modulation transfer functions shows that the response quality decreases in the following sequence: DIVCON collimator, high resolution collimator, Tomocamera and high sensitivity collimator. Although the quantitative data support the qualitative data, it is shown that the quantitative method reveals greater margins of difference and thus is a much more sensitive indicator of the response of these systems.

DD FORM 1 NOV 65 1473

UNCLASSIFIED
Security Classification